Self-organized enhancement of conductivity in biological ion channels

Self-organized enhancement of conductivity in biological ion channels

R Tindjong[1], **I Kaufman**[1], **D G Luchinsky**[1,2], **P V E McClintock**[1,5], **I Khovanov**[3] **and R S Eisenberg**[4]

[1] Department of Physics, Lancaster University, Lancaster LA1 4YB, UK
[2] Mission Critical Technologies Inc., 2041 Rosecrans Avenue, Suite 225 El Segundo, CA 90245, USA
[3] School of Engineering, University of Warwick, Coventry CV4 7AL, UK
[4] Department of Molecular Biophysics and Physiology, Rush Medical College, 1750 West Harrison, Chicago, IL 60612, USA
E-mail: r.tindjong@lancaster.ac.uk, i.kaoufman@lancaster.ac.uk, p.v.e.mcclintock@lancaster.ac.uk, dmitry.g.luchinsky@nasa.gov, I.Khovanov@warwick.ac.uk and beisenbe@rush.edu

Abstract. We discuss an example of self-organization in a biological system. It arises from long-range ion–ion interactions, and it leads us to propose a new kind of enhanced conduction in ion channels. The underlying mechanism involves charge fluctuations near the channel mouth, amplified by the mismatch between the relative permittivities of water and the protein of the channel walls. We use Brownian dynamics simulations to show that, as in conventional 'knock on' permeation, these interactions can strongly enhance the channel current; but unlike the conventional mechanism, the enhancement occurs without the instigating bath ion entering the channel. The transition between these two mechanisms is clearly demonstrated, emphasizing their distinction. A simple model accurately reproduces the observed phenomena. We point out that electrolyte plus protein of low relative permittivity are universal in living systems, so that long-range ion–ion correlations of the kind considered must be common.

[5] Author to whom any correspondence should be addressed.

IOP Institute of Physics Φ DEUTSCHE PHYSIKALISCHE GESELLSCHAFT

Contents

1. Introduction

It is well established that fluctuations (or 'noise') in nonlinear systems can lead to the appearance of important but counterintuitive phenomena. Examples include stochastic resonance [1, 2], stochastic synchronization [3, 4], stochastic ratchets [5] and the breaking of time-reversal symmetry in large fluctuations [6]. Most research in this area focuses on thermal fluctuations. But other forms of fluctuations are also possible, including the charge fluctuations that we will consider below.

The molecular processes of life occur in physiological solutions that possess binary and higher-order correlations of ionic motion. Their timescales may be very different from those of thermal fluctuations, so that they can drive the system far away from thermal equilibrium. Such a combination of thermal and non-equilibrium random fluctuations can lead to a diversity of self-organization phenomena on the molecular scale, e.g. molecular motors transforming the energy of thermal agitation into the directed motion of large molecules [5, 7] by non-equilibrium flashing of the potential between two states. There is increasing evidence pointing to the key role played by charge fluctuations in the self-organization of natural systems on the molecular scale [8–10]. Their function ranges from shaping weak intermolecular interactions [11] and effecting membrane fusion [12], to the adjustment of charged side chains within the calcium channel [13] and the blocking of channel conductance [14].

Perhaps the best-known example of the effect of ion–ion interactions on channel conductivity is the 'knock on' mechanism proposed by Hodgkin and Keynes [15]. It involves single-file movement in which an arriving ion knocks into the outermost ion within the channel, causing the trapped ion furthest from it to exit from the other side of the channel. For selective conduction, this mechanism requires (i) that the ion enters the channel and (ii) that the interacting ions be of the same species, assuming independent conduction of different types of ions. However, it is well established experimentally [16, 17] that there are deviations from this independence principle. Furthermore, channels are known to conduct ions selectively even when they are mixed with non-permeant ions of much higher concentration, as in inward-rectifying channels [18]; and they can be activated by ions of a different species, as in Ca^{2+}-activated K^+ channels [19]. It is therefore important to establish whether enhanced permeation can still occur in the absence of the restrictions (i) and (ii).

In this paper we introduce and analyse a new permeation enhancement mechanism that does not require the second ion to enter the channel and which can take advantage of interactions
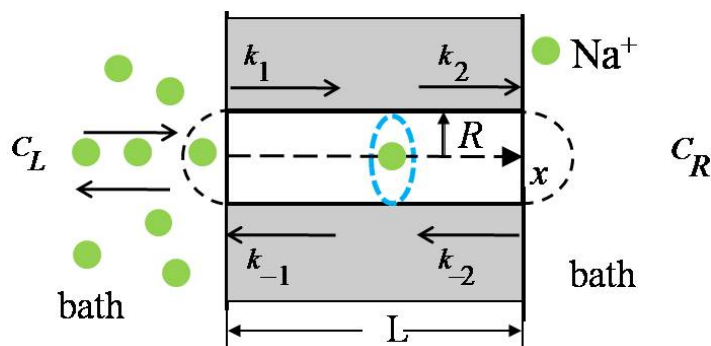
Figure 1. Simplified model of ion channel represented as a cylinder of radius R and length L. The fixed charge Q_f is represented by the blue ring at the middle of the channel.

between different species of ions. We will use Brownian dynamics (BD) simulations to show that this mechanism arises due to the strong modulation of the single-ion potential energy profile by the proximity to the channel mouth of an ion in the bath. We propose a model of this process that accurately reproduces the results of the BD simulations, distinguishes it from conventional knock on and demonstrates the transition between the two mechanisms as parameters change. We will argue that the phenomenon in question is actually a general property of conducting channels, and we will show that it appears in an archetypal model of a singly occupied channel [20, 21]. It is often assumed that an ion from the external bath cannot enter the channel if there is already an ion inside trapped at its negatively charged binding site [21], and the entry probability of the bath ion is accordingly set to zero. However, Newton's third law implies that, if the bath ion is being repelled from the channel by the ion inside the channel, then there must be an equal and opposite force tending to push the ion at the binding site on, through, and out of the channel. It is the effect of this recoil force, ignored in most earlier research, that we now explore.

In section 2 we analyse the electrostatic model of an ion channel and describe BD simulations that we have undertaken to test the theory. The results are presented in section 3 and compared with semi-analytic predictions in section 4. The transition between the new mechanism and the standard knock on mechanism is discussed in section 5. Finally, in section 6 we draw conclusions and consider the wider context.

2. Electrostatic model of an ion channel

The archetypal model [21, 22] of an ion channel views it as an open cylindrical pore of radius R and length L, through an impermeable membrane. It was shown earlier that this highly simplified model is capable of reproducing many of the key features seen in experiments on channels. More recently, it has been used [23] to predict the band structure of selectivity and conductivity in Ca^{2+} [24] and Na^+ [25] channels. It has the further advantage of allowing for the analytic calculation of channel dynamics. In this model the pore has protein walls of dielectric constant $\varepsilon_p = 2$ and it is filled with water, which is considered as a continuous dielectric of $\varepsilon_w = 80$. A single interior binding site, consisting of a ring of fixed negative charge Q_f located at x_0 as shown in figure 1. Using the model channel described in figure 1, the potential energy
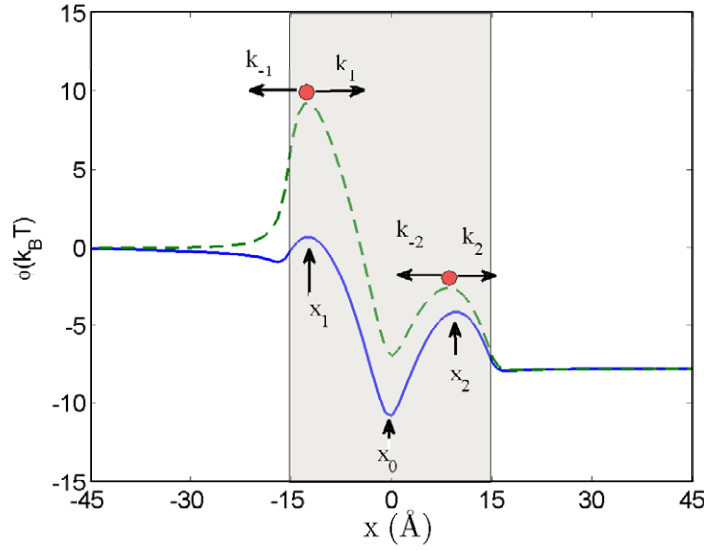
Figure 2. Potential energy profiles $\phi(x)$ for a channel with a single binding site centred on $x_0 = 0$. The full curve shows the unperturbed profile (state 1). The dashed curve shows the modified potential (state 2) due to the presence of a second ion at the channel's left mouth. The directions of the ionic transitions over the potential barriers are shown by horizontal arrows together with the escape rates k_i. The shading indicates the spatial extent of the channel, with its mouths at $\pm 15\,\text{Å}$. The escape potential barrier is located between x_0 and x_2.

profile $\phi_t(x)$ shown by the full curve in figure 2 can be calculated. We now suppose that the ionic concentrations, on the left and right of the membrane are $C_\text{L} \neq 0$ and $C_\text{R} = 0$, respectively.

We calculate the current through the channel by self-consistent solution of Poisson's equation coupled to a set of Langevin equations for N ions with coordinates x_i, mass m_i, friction coefficient γ_i and thermal energy $k_\text{B}T$. The dynamics of an ion moving in the channel potential $\phi_t(\mathbf{x}) = \phi(\mathbf{x}) + \sum_j \phi_j(\mathbf{x}, \mathbf{x}_j)$ is thus described by

$$m\gamma\dot{x} + \phi'(x) + \sum_j \phi_j'(x, x_j) = \sqrt{2m\gamma k_\text{B}T}\,\xi(t), \tag{1}$$

$$\nabla[\varepsilon_0\varepsilon\nabla(\phi_t(\mathbf{x}))] = -\sum_{i=1}^{N} z_i e\delta(\mathbf{x}_i) - e\rho_{fx}(\mathbf{x}), \tag{2}$$

where $\phi(\mathbf{x})$ is due to the protein with fixed wall charge ρ_{fx} and $\sum_j \phi_j(\mathbf{x}, \mathbf{x}_j)$ is due to the interaction with the ions in the bulk. An important feature of this model is that it includes the dielectric self-force due to the mismatch between the relative permittivities of water and the protein of the channel walls. To speed up the simulations, the potential energy of an individual ion was calculated beforehand using a two-dimensional Poisson solver [26, 27] and stored in a look-up table for all locations of that ion, thus enabling the field for an arbitrary configuration of point charges to be calculated by linear superposition [28].

The Langevin equation (1) describes the motion of an ion in the channel potential perturbed by a combination of thermal and non-equilibrium random forcing. The thermal agitation is

given by $\xi(t)$, while the random non-equilibrium modulation of the channel potential is given by $\sum_j \phi'_j(x, x_j)$. We note that the interaction with ions in the bulk electrolyte is effectively screened at the Debye screening length $\kappa^{-1} = \sqrt{\frac{e^2 n_0}{\varepsilon_w \varepsilon_0 k_B T}}$.

On account of this Debye screening, only those ions within a distance κ^{-1} from the channel mouth can affect its internal potential energy profile. For typical physiological concentrations $\kappa^{-1} \sim 5\,\text{Å}$, and the volume of the corresponding hemisphere at the channel mouth can accommodate, at most, one ion at a time. Thus the dynamics of the ion's arrival at the left mouth (and hence the potential's modulation dynamics) can be modeled as dichotomous noise [28] with an arrival time given [29] by $\tau_{ar} \propto 1/(\pi R C_L D)$ and a diffusion time away from the hemisphere $\tau_{dif} \propto R^2/3D$ [30], where the diffusion constant is defined as $D = \frac{k_B T}{m \gamma}$.

Analytic [31] and numerical [32] estimates show that the interaction between an ion at the channel mouth and the ion in the channel reduces the escape potential barrier by $\Delta \phi_{esc} \simeq 2 k_B T$. A solution of the Poisson equation demonstrating this effect for an additional ion at the channel mouth ($x = -15\,\text{Å}$) is shown by the dashed line in figure 2 (with the singularity at the mouth removed to simplify the figure). This strong modulation of the potential barrier is attributable to focusing of the electric field inside the channel [31, 32] leading to an almost linear decay of the potential along the channel axis. The latter effect can be readily understood by applying Gauss theorem to the channel interior. This can be seen by taking the control volume as a cylinder oriented along the channel axis and closed on both ends with two hemispheres. One hemisphere encompasses the ion at the channel entrance while the location of the other hemisphere is moving along the axis to the exit from the channel. Neglecting electric field leakage into the protein (which is justifiable for relatively short channels $<30\,\text{Å}$), one notices that the field at the latter hemisphere is nearly independent of its position on the axis, corresponding to the constant potential gradient of the second ion along the channel axis.

The modulation rate $w_{21} = 1/\tau_{dif}$ is of the order of the inverse relaxation time of the distribution at the binding site. Accordingly, for the ion at the binding site with coordinate x_i, the interaction term $\sum_{j \neq i} \phi'_{ij}(x_i, x_j)$ describes a random non-equilibrium modulation of the channel potential. We will show that the combination of this modulation with thermal agitation can result in a strong enhancement of the current through the channel even *without the second ion entering the channel*.

3. Results

To demonstrate this effect we solve the model (1) numerically using BD simulations and compare the solution with analytic estimates. In the simulations the ions were injected near the channel mouth at the Smoluchowski arrival rate, and allowed to diffuse along the axis. Most ions diffused away from the channel. The rare channel permeations were recorded, and the corresponding ion current was calculated. Simultaneously, we measured the time-averaged distribution of ions in the channel and the binding site occupancy p_0, defined as the probability of finding an ion near the potential minimum between x_1 and x_2 (see figure 2).

Some numerical results, obtained with diffusion coefficient $D = 1.17 \times 10^{-9}\,\text{m}^2\,\text{s}^{-1}$ in a channel of effective radius $R = 2\,\text{Å}$, length $L = 30\,\text{Å}$, fixed charge $Q_f = -0.81e$ and an external potential $200\,\text{mV}$ are shown by the open circles in figure 3(a). There is clearly a strong enhancement of the channel current for concentrations above $200\,\text{mM}$. This is preceded by the standard Michaelis–Menten type of behaviour. The dependence of the channel exit rate k_2 on

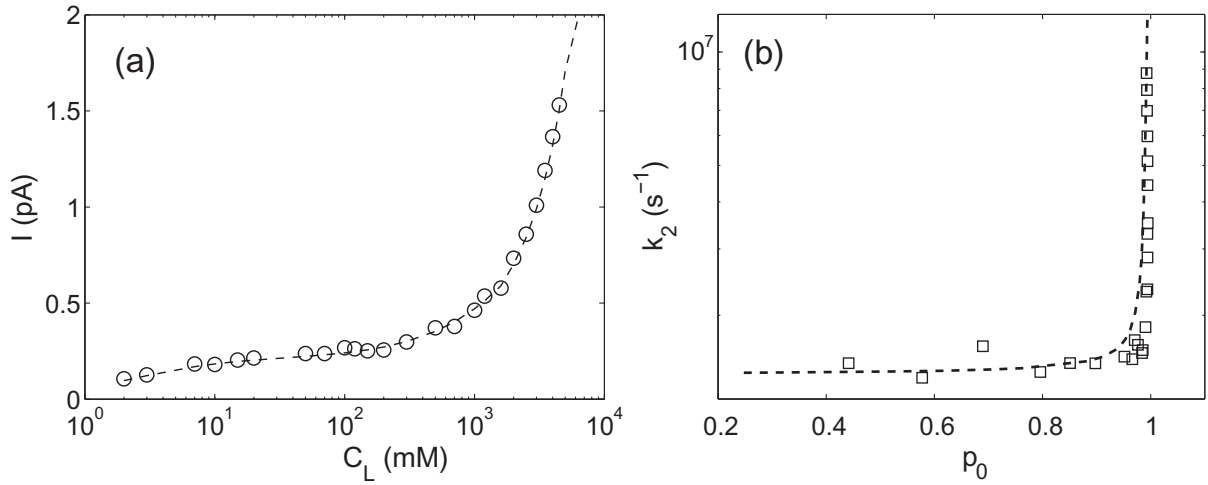**IOP** Institute of Physics ⬩ DEUTSCHE PHYSIKALISCHE GESELLSCHAFT

Figure 3. Comparisons of BD results (data points) with theory (dashed curves). (a) Current I as a function of concentration C_L. (b) Escape rate as a function of the occupation of the binding site p_0 (open squares).

the occupancy of the binding site p_0 is shown in figure 3(b). The rapid growth of current in (a) evidently corresponds to an increase of the exit rate during constant occupation (≈ 1) of the binding site.

4. Comparison with semi-analytic predictions

The dependence of the current on concentration can be understood by noting that, with zero concentration in the right-hand bath, the net current through the channel is given by $I = k_2 p_0$, where the escape rate k_2 and the occupation of the binding site p_0 can readily be calculated using non-equilibrium reaction rate (RR) theory [30] to describe the BD of an ion in a channel with a fluctuating barrier [33].

Indeed, using the RR theory it is easy to show that for $C_R = 0$ the channel occupancy is given by

$$p_0 = \frac{k_1 p_L}{k_1 p_L + k_2 + k_{-1}}. \tag{3}$$

In this equation the relationship between the rates $k_1 \gg k_2 \gg k_{-1}$ is determined by the heights of the corresponding potential barrier, while the probability of finding an ion at the left mouth is $p_L \propto C_L$.

The escape rate over the fluctuating barrier k_2 can be calculated by solving the Chapman–Kolmogorov equation [34]

$$\partial_{t'} p_i(x, t|y, t') = -A_i(y, t')\partial_y p_i(x, t|y, t') - \frac{1}{2}B_i(y, t')\partial_y^2 p_i(x, t|y, t')$$

$$+ \sum_j w_{ji}[p_j(x, t|y, t') - p_i(x, t|y, t')]. \tag{4}$$

In this equation the drift and diffusion coefficients A_i and B_i are determined by the Langevin equation in the two states with the different potential profiles ϕ shown in figure 2. Note that

$p_i(x, t|y, t')$ is not the exit probability density, but the probability density of finding the ion at time t at position x inside the channel when it started at time t' at position y (not necessarily the bottom of the potential barrier) and the potential ϕ is in state i where $i = 1$ corresponds to the potential with one ion in the channel and no ion at the left channel mouth, whereas $i = 2$ corresponds to the potential with one ion in the channel and another ion in the left channel mouth. The jumping rates between the potential states i and j are given by w_{12} and w_{21} introduced above. The exit probability density is given by the flux of p_i towards the right boundary and the quantity of interest is the mean first passage time through the right boundary. Following Gardiner [34] (see also [35]) the mean escape time $\tau(y)$ is defined as

$$T_i(y) = \int_0^\infty \int_{x_0}^{x_2} p_i(x, t|y, 0) \, dx \, dt, \tag{5}$$

where x_0 is the potential minimum and x_2 is the potential maximum close to the right mouth.

With definition (5) the solution of equation (4) can be reduced [35, 36] to the analysis of the following system of equations [30]:

$$T_1'' = \frac{1}{k_B T} \phi_1' T_1' + \omega_{21}(T_1 - T_2)/D - 1/D,$$

$$T_2'' = \frac{1}{k_B T} \phi_2' T_2' + \omega_{12}(T_2 - T_1)/D - 1/D \tag{6}$$

subject to the boundary conditions $T_i'(x = x_0, t) = 0$ and $T_i(x = x_2, t) = 0$; T_i' and T_i'' are the first and second derivatives of T_i with respect to x. The escape rate $k_2 = 1/T_1$ can then be found as a solution of the boundary value problem (6).

The equations $I = k_2 p_0$, (3) and (6) provide a semi-analytic model for both mechanisms of current enhancement: standard knock on; and the new process. Figure 3 compares the theory (dashed lines) with the BD simulations (data points) for the new process. The agreement is excellent.

For small enough C_L the arrival rate of ions to the channel is small and equations (6) are nearly decoupled. The channel potential remains unperturbed most of the time; the escape rate remains constant; and the current is determined by the variation of the binding site population p_0, which follows the Michaelis–Menten dependence on concentration C_L given by (3). It follows from the latter equation that with increase of C_L (and correspondingly p_L) the channel population approaches unity in agreement with the numerical results.

The rapid rise in channel current that occurs with further increase of C_L (and correspondingly of the modulation rate $w_{12} \propto \pi R C_L D$) shown in figure 3(a) occurs for a constant population of the binding site $p_0 \approx 1$. The current enhancement is then due entirely to the interaction of the ion at the binding site with an ion outside the channel, amplified by focusing of the electrostatic field in the channel, leading to the almost vertical dependence of the escape rate k_2 on p_0 shown in figure 3(b).

5. Transition to the standard knock on process

To determine the location of the second ion during an escape event, and to distinguish the new mechanism from standard knock on, we introduce the conditional probability $\rho(x)$ of finding a second ion in the system at position x at the moment when the first ion exits (i.e. overcomes the
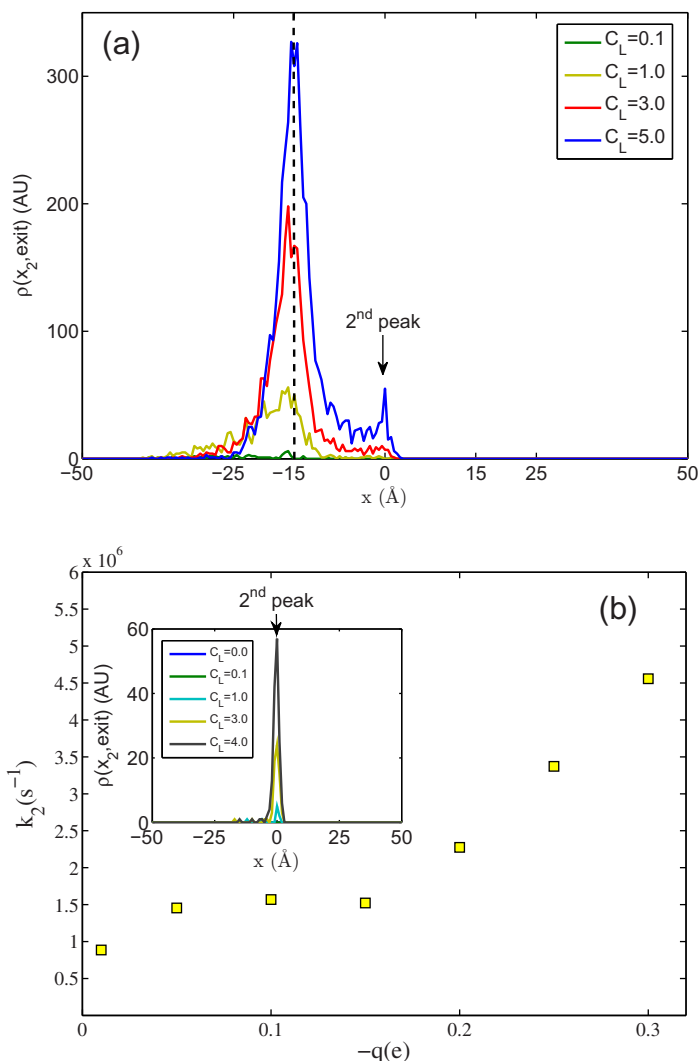
Figure 4. (a) The conditional PDF that there is a second ion at position x at the moment when the first ion escapes (without additional fixed negative charge at the mouth). (b) Escape rate k_2 as a function of the additional charge q at the mouth, calculated using BD simulations. The inset shows how the PDF in (a) is modified by increased Q_f and the presence of a mouth charge of $q = 0.05e$: the peak at the mouth has disappeared, and the second peak at the binding site ($x = 0$) is markedly enhanced.

exit potential barrier near x_2). Figure 4, which shows $\rho(x)$ normalized by the total probability of finding the ion anywhere in the system, is very revealing.

As mentioned above, standard knock on requires the second ion to enter the channel to reduce the exit potential barrier, forcing the first ion out of the channel and substituting for it at the binding site. Thus when the first ion escapes the channel, the second ion is located at the binding site with probability 1, and $\rho(x)$ will have a peak at the *channel centre* $x_0 = 0$ Å. If, on the other hand, escape takes place due to interaction with an ion in the bulk solution that does not enter the channel, $\rho(x)$ will have a peak located at the *channel mouth*.

The BD simulation results of figure 4 clearly exhibit a strong peak in the conditional probability at the channel mouth, indicating that the observed current amplification at constant p_0 takes place via the new mechanism, rather than via standard knock on. The peak appears for $C_L \gtrsim 0.2 \, \text{M}$ and increases with concentration, i.e. the current increase seen in figure 3(a) correlates strongly with the presence of a second ion at the mouth.

We observe the onset of a transition between the two mechanisms as the ionic concentration in the bulk solution increases, and the probability for the second ion to enter the channel and knock on the first ion directly becomes non-zero. Correspondingly, a second peak appears in the conditional probability distribution function (PDF) at $x = 0 \, \text{Å}$ as shown in figure 4(a).

Analysis of the dependence on Q_f of the relative probabilities of the two permeation enhancement mechanisms reveals a sharp transition to standard knock on if Q_f is increased (cf [23]). If weak additional charge q is added at the channel mouth its effect is mainly to change conduction without transition to a different mechanism. Figure 4(b) illustrates the influence of mouth charge on the escape rate k_2 for $Q_f = -1.1e$. There is a significant current increase with mouth charge. At the same time, the left-mouth peak in (a) has completely disappeared (inset) and the second peak at $x_0 = 0 \, \text{Å}$ corresponding to standard knock on has become dominant.

6. Discussion and conclusions

We have shown by semi-analytic analysis of the archetypal model, and by BD simulations, that a mechanism of enhanced conduction may exist in ion channels that differ from the standard knock on mechanism. The observed current enhancement does not require the second ion to enter the channel, and still operates even if the interacting ions are of different species. This is due to the electrostatic nature of the interaction, which does not distinguish for example between e.g. Na^+ and K^+ in the case of monovalent ions, or e.g. Ca^{2+} and Ba^{2+} in the case of divalent ions. We have found that, for a value of the fixed protein charge Q_f smaller than that required for standard knock on, this new mechanism can be dominant.

We note that, despite the highly simplified character of our archetypal model, both the current–concentration dependence shown in figure 3(a), and the dependence on the mouth charge shown in figure 4(b), are in semi-quantitative agreement with experimental observations [37] in the physiological range of parameters.

It also seems possible that the new mechanism is closely related to the 'loosely coupled knock on' process of enhanced selectivity and permeation recently observed by Corry [38] in MD simulations of the NavAb sodium channel. In this work, it was observed that the transition of Na^+ ions through the selectivity filter can be assisted by the second ion arriving at the channel mouth without entering the channel. Furthermore, in agreement with our predictions, it was shown in MD simulations that the assisting ion can be of a different type. However, further work will be needed to establish the precise connection.

More generally, because the proposed mechanism does not require the interacting ions to be of the same species, the results obtained are likely to contribute to a better understanding of the experimentally observed deviations of the equilibrium potential from predictions based on the independence principle [16, 17].

In the wider context, we note that electrolyte plus protein of low relative permittivity are always present in living systems. As here, this combination can yield long-range correlations of ionic motion comparable with thermal fluctuations in their effect on ion permeation through the complex potential landscapes that arise in molecular biology. It seems likely that such

charge fluctuations are used by the nature to organize and direct ionic motion in many different contexts.

In conclusion, calculations of permeation currents in ion channels need to take account of a permeation enhancement mechanism which, unlike standard knock on, requires neither that the bath ion enter the channel, nor that it be of the same species as the permeant ions.

Acknowledgment

References

[1] Dykman M I, Luchinsky D G, Mannella R, McClintock P V E, Stein N D and Stocks N G 1995 Stochastic resonance in perspective *Nuovo Cimento* D **17** 661–83
[2] Gammaitoni L, Hänggi P, Jung P and Marchesoni F 1998 Stochastic resonance *Rev. Mod. Phys.* **70** 223–87
[3] Van Wiggeren G D and Roy R 1998 Communication with chaotic lasers *Science* **279** 1198–200
[4] Garcia-Alvarez D, Bahraminasab A, Stefanovska A and McClintock P V E 2009 Competition between noise and coupling in the induction of synchronisation *Europhys. Lett.* **88** 30005
[5] Jülicher F, Ajdari A and Prost J 1997 Modeling molecular motors *Rev. Mod. Phys.* **69** 1269–82
[6] Luchinsky D G and McClintock P V E 1997 Irreversibility of classical fluctuations studied in analogue electrical circuits *Nature* **389** 463–6
[7] Astumian R D 2010 Thermodynamics and kinetics of molecular motors *Biophys. J.* **98** 2401–9
[8] Sung W and Kim Y 2005 How nature modulates inherent fluctuations for biological self-organization: the case of membrane fusion *J. Biol. Phys.* **31** 639–44
[9] Eisenberg B 2013 Ionic interactions are everywhere *Physiology* **28** 28–38
[10] Eisenberg B 2011 Mass action in ionic solutions *Chem. Phys. Lett.* **511** 1–6
[11] Jehle H 1957 Specificity of intermolecular forces due to quantum-mechanical and thermal charge fluctuations *Proc. Natl Acad. Sci. USA* **43** 847–55
[12] Kim Y W and Sung W 2003 Effects of charge fluctuation on two-membrane instability and fusion *Phys. Rev. Lett.* **91** 118101
[13] Giri J, Fonseca J E, Boda D, Henderson D and Eisenberg B 2011 Self-organized models of selectivity in calcium channels *Phys. Biol.* **8** 026004
[14] Nadler B, Schuss Z, Hollerbach U and Eisenberg R S 2004 Saturation of conductance in single ion channels: the blocking effect of the near reaction field *Phys. Rev.* E **70** 051912
[15] Hodgkin A L and Keynes R D 1955 The potassium permeability of a giant nerve fibre *J. Physiol.* **128** 61–88
[16] Salas P J and López E M 1982 Validity of the Goldman–Hodgkin–Katz equation in paracellular ionic pathways of gallbladder epithelium *Biochim. Biophys. Acta* **691** 178–82
[17] Weber A and Siemen D 1989 Permeability of the non-selective channel in brown adipocytes to small cations *Pflugers Arch.* **414** 564–70
[18] Hibino H, Inanobe A, Furutani K, Murakami S, Findlay I and Kurachi Y 2010 Inwardly rectifying potassium channels: their structure, function and physiological roles *Phys. Rev.* **90** 291–366
[19] Vergara C, Latorre R, Marrion N V and Adelman J P 1998 Calcium-activated potassium channels *Curr. Opin. Neurobiol.* **8** 321–9
[20] Hille B 2001 *Ion Channels of Excitable Membranes* 3rd edn (Sunderland, MA: Sinauer Associates)
[21] Aidley D J and Stanfield P R 2000 *Ion Channels: Molecules in Action* (Cambridge: Cambridge University Press)

[22] Nonner W and Eisenberg B 1998 Ion permeation and glutamate residues linked by Poisson–Nernst–Planck theory in L-type calcium channels *Biophys. J.* **75** 1287–305

[23] Kaufman I, Luchinsky D G, Tindjong R, McClintock P V E and Eisenberg R S 2013 Multi-ion conduction bands in a simple model of calcium ion channels *Phys. Biol.* **10** 026007

[24] McCleskey E W 1999 Calcium channel permeation: a field in flux *J. Gen. Physiol.* **113** 765–72

[25] Csányi É, Boda D, Gillespie D and Kristóf T 2012 Current and selectivity in a model sodium channel under physiological conditions: dynamic Monte Carlo simulations *Biochim. Biophys. Acta* **1818** 592–600

[26] Kaufman I 2009 Finite volume Poisson solver http://www.mathworks.com/matlabcentral/fileexchange/25318

[27] Oevermann M and Klein R 2006 A Cartesian grid finite volume method for elliptic equations with variable coefficients and embedded interfaces *J. Comput. Phys.* **219** 749–69

[28] Luchinsky D G, Tindjong R, Kaufman I, McClintock P V E and Eisenberg R S 2009 Charge fluctuations and their effect on conduction in biological ion channels *J. Stat. Mech.* P01010

[29] Eisenberg R S, Klosek M M and Schuss Z 1995 Diffusion as a chemical reaction: stochastic trajectories between fixed concentrations *J. Chem. Phys.* **102** 1767–80

[30] Tindjong R, Kaufman I, McClintock P V E, Luchinsky D G and Eisenberg R S 2012 Nonequilibrium rate theory for conduction in open ion channels *Fluct. Noise Lett.* **11** 1240016

[31] Cui S T 2006 Electrostatic potential in cylindrical dielectric media using the image charge method *Mol. Phys.* **104** 2993–3001

[32] Bastug T and Kuyucak S 2003 Role of the dielectric constants of membrane proteins and channel water in ion permeation *Biophys. J.* **84** 2871–82

[33] Doering C R and Gadoua J C 1992 Resonant activation over a fluctuating barrier *Phys. Rev. Lett.* **69** 2318–21

[34] Gardiner C W 2002 *Handbook of Stochastic Methods: For Physics, Chemistry and the Natural Sciences* (Berlin: Springer)

[35] Zürcher U and Doering C R 1993 Thermally activated escape over fluctuating barriers *Phys. Rev.* E **47** 3862–9

[36] Bier M and Astumian R D 1993 Matching a diffusive and a kinetic approach for escape over a fluctuating barrier *Phys. Rev. Lett.* **71** 1649–52

[37] Haug T, Sigg D, Ciani S, Toro L, Stefani E and Olcese R 2004 Regulation of K^+ flow by a ring of negative charges in the outer pore of BKCa channels: I. Aspartate 292 modulates K^+ conduction by external surface charge effect *J. Gen. Physiol.* **124** 173–84

[38] Corry B 2013 Na^+/Ca^{2+} selectivity in the bacterial voltage-gated sodium channel NavAb *PeerJ* **16** (DOI:10.7717/peerj.16)